

Crystal structure of polymeric bis(3-amino-1*H*-pyrazole)cadmium diiodide

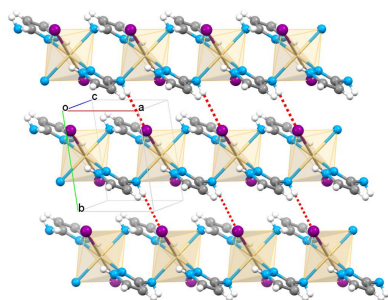
Iryna S. Kuzevanova,^{a,b} Oleksandr S. Vynohradov,^c Vadim A. Pavlenko,^c Sergey O. Malinkin,^c Sergiu Shova,^d Igor O. Fritsky^{c,b} and Maksym Seredyuk^{c*}

^aDepartment of General and Inorganic Chemistry, National Technical University of Ukraine, "Igor Sikorsky Kyiv Polytechnic Institute", Peremogy Pr. 37, Kyiv, 03056, Ukraine, ^bInnovation Development Center ABN, Pirogov str.2/37, Kyiv, 01030, Ukraine, ^cDepartment of Chemistry, Taras Shevchenko National University of Kyiv, Volodymyrska Street 64, Kyiv, 01601, Ukraine, and ^dDepartment of Inorganic Polymers, "Petru Poni" Institute of Macromolecular Chemistry, Romanian Academy of Science, Aleea Grigore Ghica Voda, 41-A, Iasi 700487, Romania. *Correspondence e-mail: mlseredyuk@gmail.com

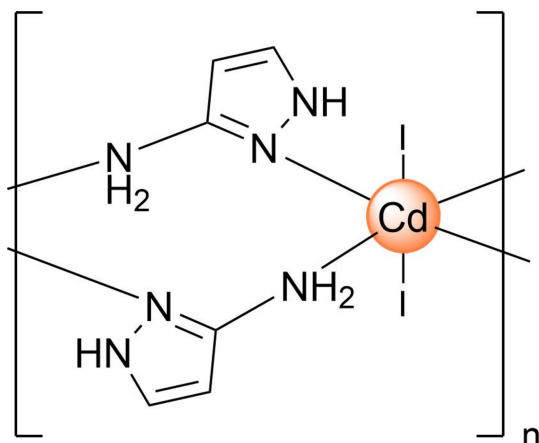
The reaction of cadmium iodide with 3-aminopyrazole (3-apz) in ethanolic solution leads to tautomerization of the ligand and the formation of crystals of the title compound, *catena*-poly[[diiiodidocadmium(II)]-bis(μ -3-amino-1*H*-pyrazole)- $\kappa^2N^2:N^3;\kappa^2N^3:N^2$], $[\text{CdI}_2(\text{C}_3\text{H}_5\text{N}_3)_2]_n$ or $[\text{CdI}_2(3\text{-apz})_2]_n$. Its asymmetric unit consists of a half of a Cd^{2+} cation, an iodide anion and a 3-apz molecule. The Cd^{2+} cations are coordinated by two iodide anions and two 3-apz ligands, generating *trans*- CdN_4I_2 octahedra, which are linked into chains by pairs of the bridging ligands. In the crystal, the ligand molecules and iodide anions of neighboring chains are linked through interchain hydrogen bonds into a diperiodic network. The intermolecular contacts were quantified using Hirshfeld surface analysis and two-dimensional fingerprint plots, revealing the relative quantitative contributions of the weak intermolecular contacts.

1. Chemical context

Inorganic–organic coordination polymers, an active field of investigation in chemistry, attract attention for their intriguing structures and applications. Inorganic components may introduce magnetic, optical, and mechanical attributes, while organic ligands offer versatility and luminescence. Combining these attributes yields novel materials with diverse properties such as catalysis, separation, luminescence, spin transition and more (Seredyuk *et al.*, 2015; Piñeiro-López *et al.*, 2021). The formation of a coordination polymer involves the self-assembly of organic ligands and metal ions, driven by strong and directional interactions such as metal–ligand coordination bonds, as well as weaker hydrogen bonds, π – π stacking, halogen–halogen, and $\text{C}–\text{H}\cdots\text{X}$ interactions ($\text{X} = \text{O}, \text{N}, \text{halogen}, \text{etc.}$). Engineering polymeric networks is a challenge that demands further exploration of metal–organic interactions. The pyrazole ligand is known to be a good linker to bind metal ions and plays a key role in the design of new functional coordination polymers. It can serve as a monodentate ligand or upon deprotonation as a bridging ligand, effectively linking metal ions into polynuclear or polymeric moieties (Parshad *et al.*, 2024). We have discovered that 3-aminopyrazole (3-apz) can form coordination polymers without the need to deprotonate the pyrazole moiety, due to the participation of the amino group in the coordination of the metal ion (Kuzevanova *et al.*, 2023). Having an interest in polymeric complexes formed by bridging ligands (Piñeiro-López *et al.*, 2018, 2021; Seredyuk *et al.*, 2007), we report here



on the coordination polymer of the apz ligand with a Cd^{2+} cation and I^- anions as co-ligands.



2. Structural commentary

The asymmetric unit comprises half of the monomeric neutral unit $[\text{Cd}(3\text{-apz})_2\text{I}_2]$, which is composed of a Cd^{2+} cation, two 3-apz bridging ligands and two I^- anions, balancing the charge (Fig. 1). The tautomerism of the ligand molecule, which can interconvert between 3- and 5-aminopyrazole in solution, is blocked, and only the first form is observed in the structure. The coordination geometry around the central ion can be described as an elongated octahedron with the I atoms being in axial positions [$\text{Cd}-\text{I1} = 2.9446(8) \text{ \AA}$] and the amino nitrogen atom of the 3-apz ligand [$\text{Cd}-\text{N1} = 2.394(9) \text{ \AA}$, $\text{Cd}-\text{N3} = 2.428(10) \text{ \AA}$] in the equatorial plane. The average trigonal distortion parameters $\Sigma = \Sigma_1^{12}(|90 - \varphi_i|)$, where φ_i is the angle $\text{N/I}-\text{Cd}-\text{N}'/\text{I}'$ (Drew *et al.*, 1995), and $\Theta = \Sigma_1^{24}(|60 - \theta_i|)$, where θ_i is the angle generated by superposition of two opposite faces of an octahedron (Chang *et al.*, 1990) are 34.0 and 140.9° , respectively. The calculated

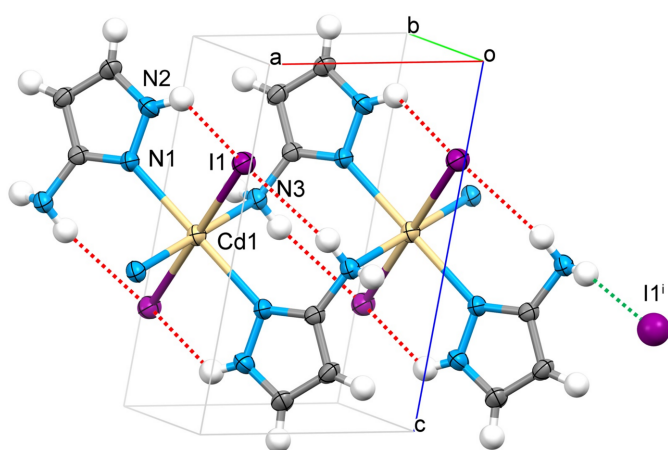


Figure 1
Crystal structure of the title compound with labeling and displacement ellipsoids drawn at the 50% probability level. The strong intra- and inter-chain $\text{N}-\text{H}\cdots\text{I}$ hydrogen bonds are shown as dashed red and green lines, respectively. Symmetry code: (i) $1 - x, -y, 1 - z$.

Table 1
Hydrogen-bond geometry ($\text{\AA}, ^\circ$).

$D-\text{H}\cdots A$	$D-\text{H}$	$\text{H}\cdots A$	$D\cdots A$	$D-\text{H}\cdots A$
$\text{N2}-\text{H2}\cdots\text{I1}$	0.86	2.96	3.526 (11)	126
$\text{N3}-\text{H3A}\cdots\text{I1}^{\text{i}}$	0.89	2.79	3.667 (10)	170
$\text{N3}-\text{H3B}\cdots\text{I1}^{\text{ii}}$	0.89	2.96	3.827 (10)	167

Symmetry codes: (i) $-x, -y + 1, -z + 1$; (ii) $x + 1, y + 1, z$.

continuous shape measure (CShM) value relative to the O_h symmetry is 1.129 (Kershaw Cook *et al.*, 2015). The values show a deviation of the coordination environment from an ideal octahedron (for which $\Sigma = \Theta = \text{CShM}(O_h) = 0$). The volume of the $[\text{CdN}_4\text{I}_2]$ coordination polyhedron is equal to 22.687 \AA^3 . The 3-apz ligand is close to planarity with a maximum deviation of $0.087(1) \text{ \AA}$ from the plane of the pyrazole ring for the amino N3 atom.

3. Supramolecular features

The $[\text{Cd}(3\text{-apz})_2\text{I}_2]$ units are linked by alternating amino/pyrazole nitrogen atoms of the 3-apz ligand to give infinite mono-periodic linear chains propagating along the a -axis direction (Figs. 1 and 2). The $\text{Cd}\cdots\text{Cd}$ distance separated by 3-aminopyrazole within the chain is $5.101(1) \text{ \AA}$. The N2 H atom and one hydrogen of the NH_2 groups of the pyrazole moiety are involved in interactions within the coordination chain, forming intrachain hydrogen bonds with the I atom. The second hydrogen atom of the NH_2 group forms a hydrogen bond with the I atom of a neighboring chain (Table 1). This interaction along the b axis expands the packing to a di-periodic supramolecular network (Fig. 2). The planes stack along the c axis with no interactions below the van der Waals radii.

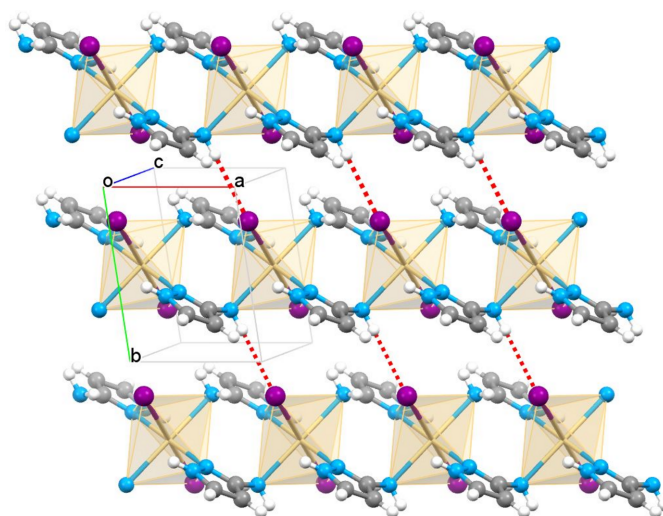


Figure 2
Fragment of the di-periodic supramolecular network formed by polymeric chains of $\{[\text{Cd}(3\text{-apz})_2\text{I}_2]\}_n$, linked by interchain $\text{N}-\text{H}\cdots\text{I}$ hydrogen bonds (red dashed lines).

4. Hirshfeld surface and two-dimensional fingerprint plots

A Hirshfeld surface analysis was performed and the associated two-dimensional fingerprint plots were generated using *CrystalExplorer* (Spackman *et al.*, 2021), with a standard resolution of the three-dimensional d_{norm} surfaces (Fig. 3*a*). Since the title compound is a coordination polymer, this analysis also includes the bonding information at the edge of the asymmetric unit. The overall two-dimensional fingerprint plot is depicted in Fig. 3*b* decomposed into specific interactions. The central spike with the tip at $(d_i, d_e) = (1.31, 1.55)$ directly represents the Cd—I bond length with a relative contribution of 2.1%, while two other closely lying spikes with

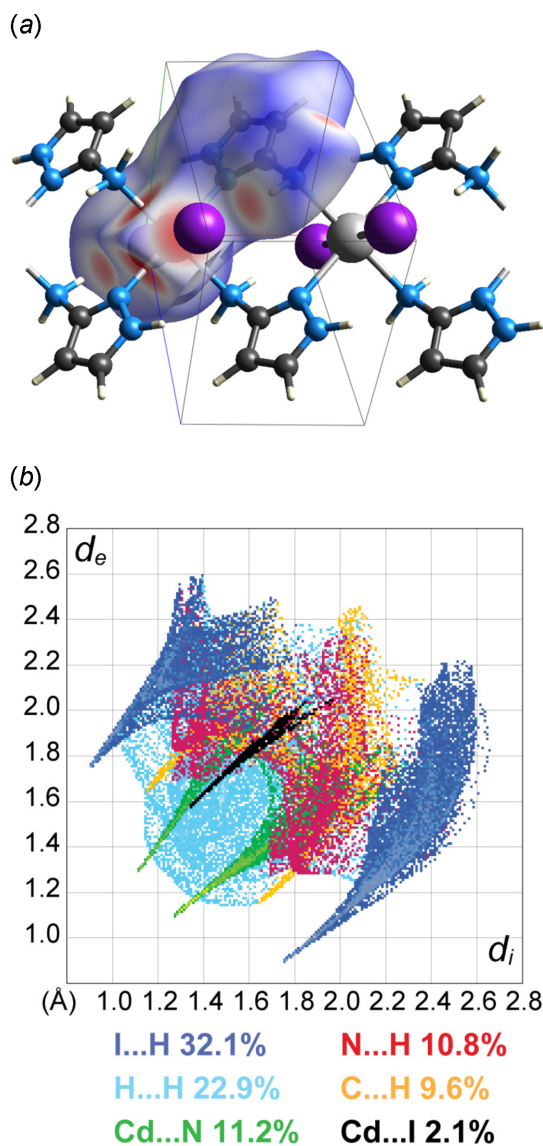


Figure 3

(*a*) A projection of d_{norm} mapped on the Hirshfeld surface onto a fragment of the polymeric chain in the asymmetric unit, visualizing the intra- and intermolecular interactions. Red/blue and white areas represent regions where contacts are shorter/longer than the sum and close to the sum of the van der Waals radii, respectively; (*b*) decomposition of the two-dimensional fingerprint plot into specific interactions.

tips at $(d_i, d_e) = (1.10, 1.30)/(1.30, 1.10)$ correspond to the shorter Cd—N bond length with a contribution of 11.2%. The rest of the contacts belong to weak hydrogen bonds. At 32.1%, the largest contribution to the overall crystal packing is from the I...H/H...I interactions, including the above discussed intra- and intermolecular contacts, which form characteristic wings of the plot with tips at $(d_i, d_e) = (0.90, 1.75)/(1.75, 0.90)$. The weak interactions, H...H (22.9%), H...C/C...H (9.6%) and H...N/N...H (10.8%), are mainly distributed in the middle part of the plot.

5. Database survey

A search of the Cambridge Structural Database (CSD version 5.43, update of November 2022; Groom *et al.*, 2016) reveals one hit with a 3-apz bridging ligand in a binuclear Cu^{2+} complex TIXDAH with oxalyl anions as coligands (Świtlicka-Olszewska *et al.*, 2014) and another hit for a binuclear Co^{2+} complex FAZCIW with 6-phenylpyridine-2-carboxylic acid as coligands (Xiang & Xi-Shi, 2022). In both complexes, the same bridging coordination mode of the ligand is observed, but with a shorter intermetallic separation than in the title compound (4.583 Å for the Cu^{2+} complex and 4.728 Å for the Co^{2+} complex), which is due to the different chemical nature and coordination geometry of the central ions. Comparison with the recently reported isomorphous compound $\{[\text{Cd}(3\text{-apz})_2]\text{Br}_2\}_n$ (Kuzevanova *et al.*, 2023) shows that the larger unit-cell parameters in the title compound are due solely to the larger iodine atoms. In addition, the larger Cd—I distance leads to increasing distortion indices of the coordination polyhedron compared to the isomorphous compound.

6. Synthesis and crystallization

CdI_2 and 3-apz were purchased from Sigma Aldrich and were used without further purification. Colorless block-like crystals were obtained by the reaction of 1 mmol of CdI_2 (366 mg) and 2 mmol of 3-apz (166 mg) in 10 ml of ethanol (96%). The reaction mixture was left overnight in an open vial, leading to the formation of crystals suitable for single-crystal X-ray analysis (404 mg, 76%). Elemental analysis calculated for $\text{C}_6\text{H}_{10}\text{I}_2\text{CdN}_6$: C, 13.54; H, 1.89; N, 15.79. Found: C, 13.57; H, 1.98; N, 15.30. IR (KBr; cm^{-1}): 3322(*s*) $\nu(\text{NH})$; 1589 (*m*), 1552(*m*) and 1536(*s*) $\nu(\text{C}=\text{N}/\text{C}_{3\text{-apz}})$.

7. Refinement

Crystal data, data collection and structure refinement details are summarized in Table 2. H atoms were refined as riding [$\text{C}-\text{H} = 0.83\text{--}0.92$ Å with $U_{\text{iso}}(\text{H}) = 1.2U_{\text{eq}}(\text{C}/\text{N})$]. Twinning was detected using *CrysAlis PRO* 1.171.42.93a software, with the second twin component obtained by rotation of 180° around $[0.00\ 0.00\ 1.00]$ in reciprocal space. The content of component 1 was refined to be 0.8775 (14); the content of component 2 was refined to be 0.1225 (14). The hkl4 and hkl5 files were generated using *CrysAlis PRO* 1.171.42.93a. The highest peak of 2.00 is 1.51 Å from C3 and the deepest hole of

1.92 is 0.87 Å from I1. There are 13 reflections omitted from the refinement for which the error/e.s.d. ratio was over 10.

Acknowledgements

Author contributions are as follows: Conceptualization, VAP and IOF; methodology, OSV; formal analysis, SOM; synthesis, ISK, OSV; single-crystal measurements, SS; writing (original draft), MS; writing (review and editing of the manuscript), SOM, MS; visualization and calculations, MS; funding acquisition, MS, IOF.

Funding information

Funding for this research was provided by: the Ministry of Education and Science of Ukraine (grant Nos. 22BF037-03, 22BF037-04, 22BF037-09, 24BF037-03) .

References

Chang, H. R., McCusker, J. K., Toftlund, H., Wilson, S. R., Trautwein, A. X., Winkler, H. & Hendrickson, D. N. (1990). *J. Am. Chem. Soc.* **112**, 6814–6827.

Dolomanov, O. V., Bourhis, L. J., Gildea, R. J., Howard, J. A. K. & Puschmann, H. (2009). *J. Appl. Cryst.* **42**, 339–341.

Drew, M. G. B., Harding, C. J., McKee, V., Morgan, G. G. & Nelson, J. (1995). *J. Chem. Soc. Chem. Commun.* pp. 1035–1038.

Groom, C. R., Bruno, I. J., Lightfoot, M. P. & Ward, S. C. (2016). *Acta Cryst.* **B72**, 171–179.

Kershaw Cook, L. J., Mohammed, R., Sherborne, G., Roberts, T. D., Alvarez, S. & Halcrow, M. A. (2015). *Coord. Chem. Rev.* **289–290**, 2–12.

Kuzevanova, I. S., Vynohradov, O. S., Pavlenko, V. A., Malinkin, S. O., Shova, S., Fritsky, I. O. & Seredyuk, M. (2023). *Acta Cryst.* **E79**, 1151–1154.

Parshad, M., Kumar, D. & Verma, V. (2024). *Inorg. Chim. Acta*, **560**, 121789.

Piñeiro-López, L., Valverde-Muñoz, F. J., Seredyuk, M., Bartual-Murgui, C., Muñoz, M. C. & Real, J. A. (2018). *Eur. J. Inorg. Chem.* pp. 289–296.

Piñeiro-López, L., Valverde-Muñoz, F.-J., Trzop, E., Muñoz, M. C., Seredyuk, M., Castells-Gil, J., da Silva, I., Martí-Gastaldo, C., Collet, E. & Real, J. A. (2021). *Chem. Sci.* **12**, 1317–1326.

Rigaku (2023). *CrysAlis PRO*. Rigaku Oxford Diffraction, Yarnton, England.

Table 2

Experimental details.

Crystal data	
Chemical formula	[CdI ₂ (C ₃ H ₅ N ₃) ₂]
<i>M_r</i>	532.40
Crystal system, space group	Triclinic, <i>P</i> $\bar{1}$
Temperature (K)	293
<i>a</i> , <i>b</i> , <i>c</i> (Å)	5.1007 (1), 6.9544 (2), 9.0470 (4)
α , β , γ (°)	83.198 (3), 79.962 (3), 81.742 (2)
<i>V</i> (Å ³)	311.29 (2)
<i>Z</i>	1
Radiation type	Mo <i>K</i> α
μ (mm ⁻¹)	6.69
Crystal size (mm)	0.25 × 0.25 × 0.15
Data collection	
Diffractometer	XtaLAB Synergy, Dualflex, HyPix
Absorption correction	Multi-scan (<i>CrysAlis PRO</i> ; Rigaku OD, 2023)
<i>T_{min}</i> , <i>T_{max}</i>	0.725, 1.000
No. of measured, independent and observed [<i>I</i> > 2 σ (<i>I</i>)] reflections	5468, 5468, 4327
<i>R_{int}</i>	0.050
(<i>sin</i> θ / λ) _{max} (Å ⁻¹)	0.722
Refinement	
<i>R</i> [<i>F</i> ² > 2 σ (<i>F</i> ²)], <i>wR</i> (<i>F</i> ²), <i>S</i>	0.050, 0.170, 1.17
No. of reflections	5468
No. of parameters	72
H-atom treatment	H-atom parameters constrained
$\Delta\rho_{\max}$, $\Delta\rho_{\min}$ (e Å ⁻³)	2.00, -1.92

Computer programs: *CrysAlis PRO* (Rigaku OD, 2023), *SHELXT* (Sheldrick, 2015a), *SHELXL2018/3* (Sheldrick, 2015b) and *OLEX2* 1.5 (Dolomanov *et al.*, 2009).

Seredyuk, M., Haukka, M., Fritsky, I. O., Kozłowski, H., Krämer, R., Pavlenko, V. A. & Gütllich, P. (2007). *Dalton Trans.* pp. 3183–3194.

Seredyuk, M., Piñeiro-López, L., Muñoz, M. C., Martínez-Casado, F. J., Molnár, G., Rodríguez-Velamazán, J. A., Bousseksou, A. & Real, J. A. (2015). *Inorg. Chem.* **54**, 7424–7432.

Sheldrick, G. M. (2015a). *Acta Cryst.* **A71**, 3–8.

Sheldrick, G. M. (2015b). *Acta Cryst.* **C71**, 3–8.

Spackman, P. R., Turner, M. J., McKinnon, J. J., Wolff, S. K., Grimwood, D. J., Jayatilaka, D. & Spackman, M. A. (2021). *J. Appl. Cryst.* **54**, 1006–1011.

Świtlicka-Olszewska, A., Machura, B., Mroziński, J., Kalińska, B., Kruszynski, R. & Penkala, M. (2014). *New J. Chem.* **38**, 1611–1626.

Xiang, G. & Xi-Shi, T. (2022). *Z. Kristallogr. New Cryst. Struct.* **237**, 421–423.

supporting information

Acta Cryst. (2024). E80 [https://doi.org/10.1107/S2056989024006418]

Crystal structure of polymeric bis(3-amino-1*H*-pyrazole)cadmium diiodide

Iryna S. Kuzevanova, Oleksandr S. Vynohradov, Vadim A. Pavlenko, Sergey O. Malinkin, Sergiu Shova, Igor O. Fritsky and Maksym Seredyuk

Computing details

catena-Poly[[diiodidocadmium(II)]-bis(μ -3-amino-1*H*-pyrazole)- κ^2 N²:N³; κ^2 N³:N²]

Crystal data

[CdI₂(C₃H₅N₃)₂]

$M_r = 532.40$

Triclinic, $P\bar{1}$

$a = 5.1007$ (1) Å

$b = 6.9544$ (2) Å

$c = 9.0470$ (4) Å

$\alpha = 83.198$ (3)°

$\beta = 79.962$ (3)°

$\gamma = 81.742$ (2)°

$V = 311.29$ (2) Å³

$Z = 1$

$F(000) = 242$

$D_x = 2.840$ Mg m⁻³

Mo $K\alpha$ radiation, $\lambda = 0.71073$ Å

Cell parameters from 5030 reflections

$\theta = 3.0$ – 30.1 °

$\mu = 6.69$ mm⁻¹

$T = 293$ K

Block, colourless

$0.25 \times 0.25 \times 0.15$ mm

Data collection

XtaLAB Synergy, Dualflex, HyPix
diffractometer

Radiation source: micro-focus sealed X-ray
tube, PhotonJet (Mo) X-ray Source

Mirror monochromator

Detector resolution: 10.0000 pixels mm⁻¹

ω scans

Absorption correction: multi-scan
(CrysAlisPro; Rigaku OD, 2023)

$T_{\min} = 0.725$, $T_{\max} = 1.000$

5468 measured reflections

5468 independent reflections

4327 reflections with $I > 2\sigma(I)$

$R_{\text{int}} = 0.050$

$\theta_{\max} = 30.9$ °, $\theta_{\min} = 3.0$ °

$h = -7 \rightarrow 6$

$k = -9 \rightarrow 9$

$l = -12 \rightarrow 12$

Refinement

Refinement on F^2

Least-squares matrix: full

$R[F^2 > 2\sigma(F^2)] = 0.050$

$wR(F^2) = 0.170$

$S = 1.17$

5468 reflections

72 parameters

0 restraints

Primary atom site location: dual

Hydrogen site location: inferred from
neighbouring sites

H-atom parameters constrained

$w = 1/[\sigma^2(F_o^2) + (0.0542P)^2 + 4.3767P]$

where $P = (F_o^2 + 2F_c^2)/3$

$(\Delta/\sigma)_{\max} < 0.001$

$\Delta\rho_{\max} = 2.00$ e Å⁻³

$\Delta\rho_{\min} = -1.92$ e Å⁻³

Extinction correction: *SHELXL2018/3*

(Sheldrick, 2015b),

$F_c^* = kFc[1 + 0.001xFc^2\lambda^3/\sin(2\theta)]^{-1/4}$

Extinction coefficient: 0.022 (4)

Special details

Geometry. All esds (except the esd in the dihedral angle between two l.s. planes) are estimated using the full covariance matrix. The cell esds are taken into account individually in the estimation of esds in distances, angles and torsion angles; correlations between esds in cell parameters are only used when they are defined by crystal symmetry. An approximate (isotropic) treatment of cell esds is used for estimating esds involving l.s. planes.

Refinement. Refined as a 2-component twin.

Fractional atomic coordinates and isotropic or equivalent isotropic displacement parameters (\AA^2)

	<i>x</i>	<i>y</i>	<i>z</i>	$U_{\text{iso}}^*/U_{\text{eq}}$
I1	−0.05344 (17)	0.22724 (12)	0.28482 (9)	0.0357 (3)
Cd1	0.000000	0.500000	0.500000	0.0278 (4)
N3	0.6523 (19)	0.7498 (15)	0.4240 (11)	0.028 (2)
H3A	0.520223	0.759070	0.502295	0.034*
H3B	0.720382	0.862672	0.408825	0.034*
N1	0.3258 (19)	0.6357 (16)	0.3078 (11)	0.030 (2)
N2	0.282 (2)	0.6411 (17)	0.1627 (11)	0.034 (2)
H2	0.156052	0.589059	0.136826	0.041*
C3	0.535 (2)	0.7342 (16)	0.2968 (12)	0.025 (2)
C1	0.458 (2)	0.7361 (19)	0.0661 (14)	0.034 (3)
H1	0.464247	0.756161	−0.037912	0.041*
C2	0.628 (2)	0.7995 (18)	0.1459 (13)	0.032 (2)
H2A	0.771493	0.869483	0.109148	0.038*

Atomic displacement parameters (\AA^2)

	U^{11}	U^{22}	U^{33}	U^{12}	U^{13}	U^{23}
I1	0.0408 (5)	0.0388 (5)	0.0311 (5)	−0.0160 (3)	−0.0036 (3)	−0.0083 (3)
Cd1	0.0268 (6)	0.0331 (6)	0.0253 (6)	−0.0094 (4)	−0.0057 (4)	−0.0013 (4)
N3	0.025 (5)	0.034 (5)	0.028 (5)	−0.007 (4)	−0.006 (4)	−0.005 (4)
N1	0.028 (5)	0.042 (6)	0.024 (5)	−0.015 (4)	−0.005 (4)	−0.002 (4)
N2	0.036 (5)	0.046 (6)	0.026 (5)	−0.015 (5)	−0.012 (4)	0.000 (4)
C3	0.027 (5)	0.025 (5)	0.023 (5)	−0.005 (4)	−0.002 (4)	−0.002 (4)
C1	0.034 (6)	0.037 (6)	0.030 (6)	−0.013 (5)	−0.006 (5)	0.009 (5)
C2	0.029 (6)	0.035 (6)	0.029 (6)	−0.009 (5)	0.002 (4)	0.003 (5)

Geometric parameters (\AA , $^\circ$)

I1—Cd1	2.9446 (8)	N1—N2	1.364 (13)
Cd1—N3 ⁱ	2.428 (10)	N1—C3	1.330 (14)
Cd1—N3 ⁱⁱ	2.428 (10)	N2—H2	0.8600
Cd1—N1 ⁱⁱⁱ	2.394 (9)	N2—C1	1.328 (15)
Cd1—N1	2.394 (9)	C3—C2	1.409 (16)
N3—H3A	0.8900	C1—H1	0.9300
N3—H3B	0.8900	C1—C2	1.367 (18)
N3—C3	1.409 (14)	C2—H2A	0.9300
I1 ⁱⁱⁱ —Cd1—I1	180.00 (2)	C3—N3—Cd1 ^{iv}	120.7 (7)

N3 ⁱⁱ —Cd1—I1	95.4 (2)	C3—N3—H3A	107.1
N3 ⁱ —Cd1—I1	84.6 (2)	C3—N3—H3B	107.1
N3 ⁱ —Cd1—I1 ⁱⁱⁱ	95.4 (2)	N2—N1—Cd1	116.6 (7)
N3 ⁱⁱ —Cd1—I1 ⁱⁱⁱ	84.6 (2)	C3—N1—Cd1	138.7 (8)
N3 ⁱ —Cd1—N3 ⁱⁱ	180.0 (4)	C3—N1—N2	104.1 (9)
N1 ⁱⁱⁱ —Cd1—I1 ⁱⁱⁱ	87.2 (2)	N1—N2—H2	124.0
N1 ⁱⁱⁱ —Cd1—I1	92.8 (2)	C1—N2—N1	112.0 (10)
N1—Cd1—I1	87.2 (2)	C1—N2—H2	124.0
N1—Cd1—I1 ⁱⁱⁱ	92.8 (2)	N1—C3—N3	121.2 (10)
N1 ⁱⁱⁱ —Cd1—N3 ⁱ	90.3 (3)	N1—C3—C2	111.6 (10)
N1 ⁱⁱⁱ —Cd1—N3 ⁱⁱ	89.7 (3)	C2—C3—N3	126.9 (10)
N1—Cd1—N3 ⁱⁱ	90.3 (3)	N2—C1—H1	125.9
N1—Cd1—N3 ⁱ	89.7 (3)	N2—C1—C2	108.2 (10)
N1 ⁱⁱⁱ —Cd1—N1	180.0	C2—C1—H1	125.9
Cd1 ^{iv} —N3—H3A	107.1	C3—C2—H2A	128.0
Cd1 ^{iv} —N3—H3B	107.1	C1—C2—C3	104.0 (10)
H3A—N3—H3B	106.8	C1—C2—H2A	128.0
Cd1 ^{iv} —N3—C3—N1	86.6 (12)	N1—N2—C1—C2	-0.3 (15)
Cd1 ^{iv} —N3—C3—C2	-87.2 (13)	N1—C3—C2—C1	0.9 (14)
Cd1—N1—N2—C1	173.7 (9)	N2—N1—C3—N3	-175.7 (10)
Cd1—N1—C3—N3	14.0 (19)	N2—N1—C3—C2	-1.0 (13)
Cd1—N1—C3—C2	-171.4 (9)	N2—C1—C2—C3	-0.4 (14)
N3—C3—C2—C1	175.2 (11)	C3—N1—N2—C1	0.8 (14)

Symmetry codes: (i) $-x+1, -y+1, -z+1$; (ii) $x-1, y, z$; (iii) $-x, -y+1, -z+1$; (iv) $x+1, y, z$.

Hydrogen-bond geometry ($\text{\AA}, ^\circ$)

$D-H\cdots A$	$D-H$	$H\cdots A$	$D\cdots A$	$D-H\cdots A$
N2—H2 \cdots I1	0.86	2.96	3.526 (11)	126
N3—H3A \cdots I1 ⁱⁱⁱ	0.89	2.79	3.667 (10)	170
N3—H3B \cdots I1 ^v	0.89	2.96	3.827 (10)	167

Symmetry codes: (iii) $-x, -y+1, -z+1$; (v) $x+1, y+1, z$.